Aluminum Oxynitride Capacitors for Multilayer Devices with Higher Energy Density and Wide Temperature Properties

Kevin R. Bray
K Systems Corp.
1522 Marsetta Dr.
Beavercreek, OH 45432
1-937-255-6545
1-937-255-3211 fax
kevin.bray@wpafb.af.mil

Richard L.C. Wu
K Systems Corp.
1522 Marsetta Dr.
Beavercreek, OH 45432
1-937-255-6933
1-937-255-3211 fax
richard.wu@wpafb.af.mil

Sandra Fries-Carr
Air Force Research Laboratory, AFRL/PRPE
Wright Patterson AFB, OH 45433

Joseph Weimer
Air Force Research Laboratory, AFRL/PRPE
Wright Patterson AFB, OH 45433

Abstract

Capacitors are a critical technology in numerous applications. Increased performance and smaller size in capacitor devices have been the main focus of our research in the development of new dielectrics. A multilayer stacked rigid aluminum oxynitride (AlON) capacitor design concept has been developed to improve the energy density and high temperature capability of AlON capacitors. This method consists of depositing alternating layers of dielectric and metal on a rigid substrate. Thin clearable metal electrodes are evaluated in device performance. Dielectric defects are cleared without significant loss of capacitance. Thinner electrodes exhibit less energy during clearing. Amorphous aluminum oxynitride films possess unique properties of high dielectric strength, high resistivity, low loss, high decomposition

temperature, chemical inertness and good thermal conductivity. Dual DC pulsed magnetron reactive sputtering was employed to synthesize amorphous AlON films on various substrates. Dielectric properties were compared for films developed with different process conditions. The properties were optimized with respect to the following input parameters: DC power, pulse frequency, total pressure, substrate temperature and reactive gas ratio. Initial effects on the dielectric constant, frequency dependence of capacitance, dissipation factor, resistivity, and breakdown strength of these films were measured using simple parallel plate capacitor test structures. Larger area single and multilayer devices were constructed using an in-situ process. Temperature dependent dielectric properties were evaluated from -200˚C to 400°C

Introduction

High Power Density Capacitors

Capacitors are key components in all forms of electrical devices. Numerous applications utilize millions of capacitors and consider them key components due to their susceptibility for failure. Future applications require the development of compact, high energy density capacitors for high power and extreme environment applications. Current applications are dominated by polymer film capacitors. Available state-of-the-art (SOTA) dielectric materials include polymer films such as polypropylene (PP), polyester (PET) and polyvinylidene fluoride (PVdF)[1]. Polymers are used for most AC applications because of their non-polar nature and low dielectric losses. Key drawbacks to polymer films include their low operating temperature, typically ~100°C[1], and their large volume-to-weight ratio, which compromises energy storage density.

Most polymers also have a dielectric constant (k) in the range of 2 – 4, although k for PVdF is from 10 – 12 [1]. These low k values make it difficult to obtain the high energy density required for future military applications. Polymer breakdown voltage is typically ~550 V/ m[1]. Energy density (u_v) depends linearly on dielectric constant (k) and on the square of the breakdown strength (E_B) of a capacitor as shown in Equation 1,

$$u_v = \frac{1}{2} k \;\; _{o}E_B^{2} \qquad (1)$$

where $_o$ is the permittivity of free space. Increasing the breakdown voltage increases the energy density more rapidly than increasing the dielectric constant. Current SOTA polymer dielectrics achieve material energy densities between 3 and 10 J/cc. Improved dielectric materials for capacitors are needed to meet the military's future power applications. Materials with a higher dielectric constant, greater dielectric breakdown strength and superior thermal stability are needed to improve capacitor performance to meet emerging needs.

Aluminum Oxynitride Dielectrics

Crystalline aluminum nitride (AlN) is a semiconductor with one of the largest known bandgaps (6.2 eV)[2,3] with dielectric strength between 400 and 550 V/ m[4] and thermal conductivity from 320 W/mK [3]. Amorphous AlN retains many of the crystalline properties and the insulating properties and high resistivity in conjunction with the high breakdown strength make amorphous AlN a desirable material for high density power applications. Thin AlN films have been deposited using a wide range of processes including MOCVD[5,6], RF and DC magnetron sputtering[4,7,8,9,10], and pulsed laser deposition[3,10]. Film structures from amorphous to epitaxial crystals have been obtained by varying deposition parameters and substrates[11]. Pulsed DC sputter deposition produces faster deposition rates than other

deposition methods and also results in less substrate heating and thermal stressing of the films[9]. The aluminum target does not experience the same target poisoning that occurs during Al_2O_3 sputtering, making the AlN process easier to control and reproduce[8]. Thin amorphous Al_2O_3 films have shown breakdown strength ~500 V/ m[12]. Aluminum oxynitride deposition utilizing DC pulsed magnetron sputtering is a stable, repeatable process. Thin films deposited from this method show breakdown strengths ~600 V/ m[13,14].

Stacked Multilayer Capacitors

Multilayer capacitor configurations are a well established technology for increasing the energy density of a capacitor device. Multilayer construction can increase the energy density by up to ten times compared to conventional single layer capacitor fabrication[15]. The large increase in energy density comes from the removal of the inert, volume-filling carrier material. Further reduction of the metal layer thickness in the stack will additionally increase the energy density towards its theoretical limits. Thin film multilayered capacitors also reduce processing issues arising from the film stress and wrinkling associated with depositing thin dielectric films on very thin polymeric and foil substrates for rolled structures. Multilayer capacitors are also more compatible with surface mount technology than rolled capacitors. Multilayer devices do typically have a drawback with higher inductance and effective series resistance than single layer capacitors.

Experimental

Film Synthesis

Amorphous aluminum nitride films were deposited using a pulsed DC magnetron sputtering technique. The chamber was pumped to a base pressure less than $5x10^{-6}$ Torr before deposition. DC power was varied from 500 – 2000 W with pulse frequencies from 25 – 250 kHz. Films were deposited using pure nitrogen, nitrogen/oxygen and nitrogen/nitrous oxide gas mixtures with 99.999% pure aluminum sputter targets. Gas pressures ranged from 3 mTorr to 20 mTorr. Deposition conditions strongly influence the crystallinity of the films[16], but optical and secondary electron microscopy observation confirmed our films were amorphous under the deposition conditions examined. The target-to-substrate spacing was adjusted to influence substrate heating and film uniformity with an optimal distance of 3 inches used for the majority of the runs. The target was conditioned before each run using argon plasma to remove contamination from the surface. Deposition times were adjusted to achieve ~5000 Å films. Thicknesses were verified using profilometry. Parallel plate capacitors were constructed by evaporating 3 mm diameter dots on the top surface of the deposited films through a shadow mask for initial film characterization. Larger area single and multilayer capacitors were formed for more in-depth evaluation.

Multilayer Capacitor Fabrication

Multilayer capacitor structures were deposited using in-situ processing. A wafer transfer manipulator was used to precisely position the substrate behind shadow masks. The pulsed magnetron system was employed to deposit metal contacts from an argon plasma and oxynitride dielectric layers from a nitrous oxide gas mixture in the same chamber. Separate targets were employed for the metal and dielectric deposition. Targets were presputtered before deposition to remove contamination from the surface.

Dielectric Property Evaluation

Capacitance and dissipation factors were measured as a function of frequency using an LCR meter. Multiple measurements were taken at each frequency and averaged for the capacitor.

Several capacitors were tested on each film to confirm uniformity across the material. The dielectric constant was calculated using the average capacitance value at 1 kHz and the measured thickness for each film. The capacitance and dissipation factor were also measured at elevated and cryogenic temperatures. The dielectric breakdown strength was measured using an electrometer. Breakdown voltage was determined by applying a voltage stepped in regular increments to a capacitor for set time durations and measuring the resulting leakage current until film failure occurred.

Results and Discussion

Dielectric Properties

Single layer capacitor devices were constructed with an in-situ deposition process. Figure 1 plots the capacitance vs. frequency. The capacitance remains constant up to 50 kHz, and then begins to drop. A dielectric constant of ~9 is obtained. The dissipation factor is shown in Figure 2. It is below 1% at 1kHz. Dielectric breakdown strength is a critical parameter in obtaining high energy density and the dissipation factor is a key indicator of losses in the material. Dielectric breakdown strengths ~650 V/ m have been achieved and will be discussed more in reference to electrode clearing below.

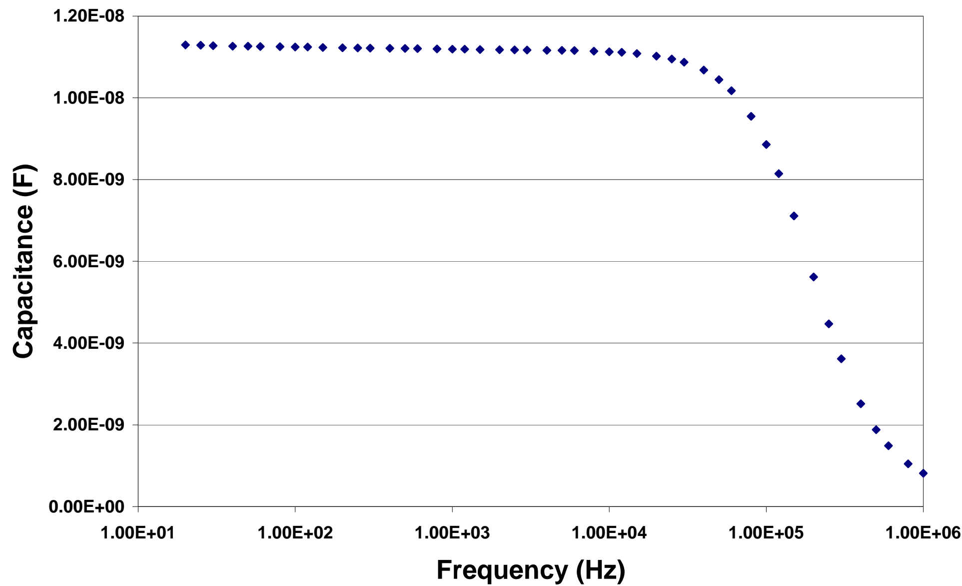

Figure 1. Capacitance vs. frequency for single layer AlON capacitor.

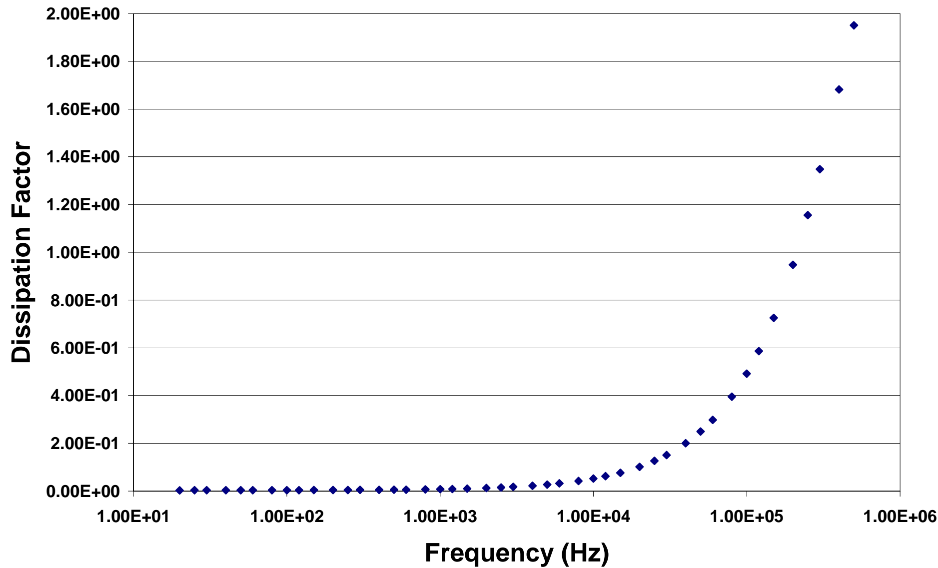

Figure 2. Dissipation factor vs. frequency for single layer AlON capacitor

<u>Clearing</u>

Thin aluminum electrodes of 100Å or less were deposited to form capacitor structures. The thin metal allows the capacitor to clear to increase the breakdown voltage. Figure 3 plots the leakage current through the capacitor and the capacitance vs. the applied voltage for two single layer devices. The leakage increases relatively smoothly until there are some sharp spikes around 350V and 450V. The capacitance remains constant with voltage until 350V and 450V respectively. A significant drop in capacitance is observed at these voltages which correspond with the spikes in the leakage current. Figure 4 shows optical images of the capacitor surface after applied voltages from 0V to 350V. Images (a) – (f) depict the surface from as deposited to 250V. No effects from the voltage are visible. One major clearing site is visible if Figure 4(g) at 300V, but it does not affect the overall capacitance of the device as seen in Figure 3. As the voltage is ramped further, another clearing event is observed (not shown) immediately adjacent to the previous site and most apparently resulting from damage during the previous clearing and not inherent defects in the material. The breakdown test was restarted again from 350V and the capacitor lost contact almost immediately. Figure 4(h) shows the edge of the electrode. A series of clearing events propagated out from the previous damage and cut off the electrode. The appearance of the clearing damage to the surface is very different between the early events seen in Fig. 4(g) and the damage seen in Fig. 4(h). The clearing in Figure 4(h) spread across the whole edge almost simultaneously, unlike the previous isolated clearings. This suggests that the original clearing was caused by a defect or pinhole in the dielectric which resulted in self-healing of the capacitor with no significant loss of capacitance. The smaller, more rapid clearing is concentrated on the edge of the electrode and most likely results from the enhanced field effect in the device. This rapid clearing causes the device to lose contact with the electrode at ~600 V/ m, but the dielectric has still not broken down under this voltage. Thinner metal electrodes were also examined. A 50Å aluminum electrode did not provide sufficient continuity for the capacitor to hold charge. High temperature titanium was also evaluated. The sputtering process did

not produce a uniform metal film and a different approach may be needed for commercial metallization.

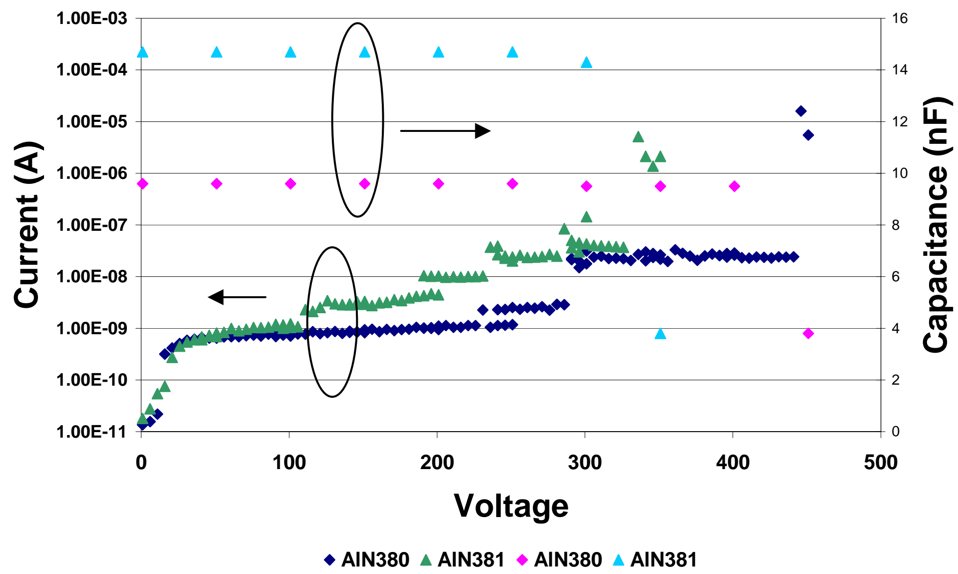

Figure 3. Capacitance and leakage vs. applied voltage.

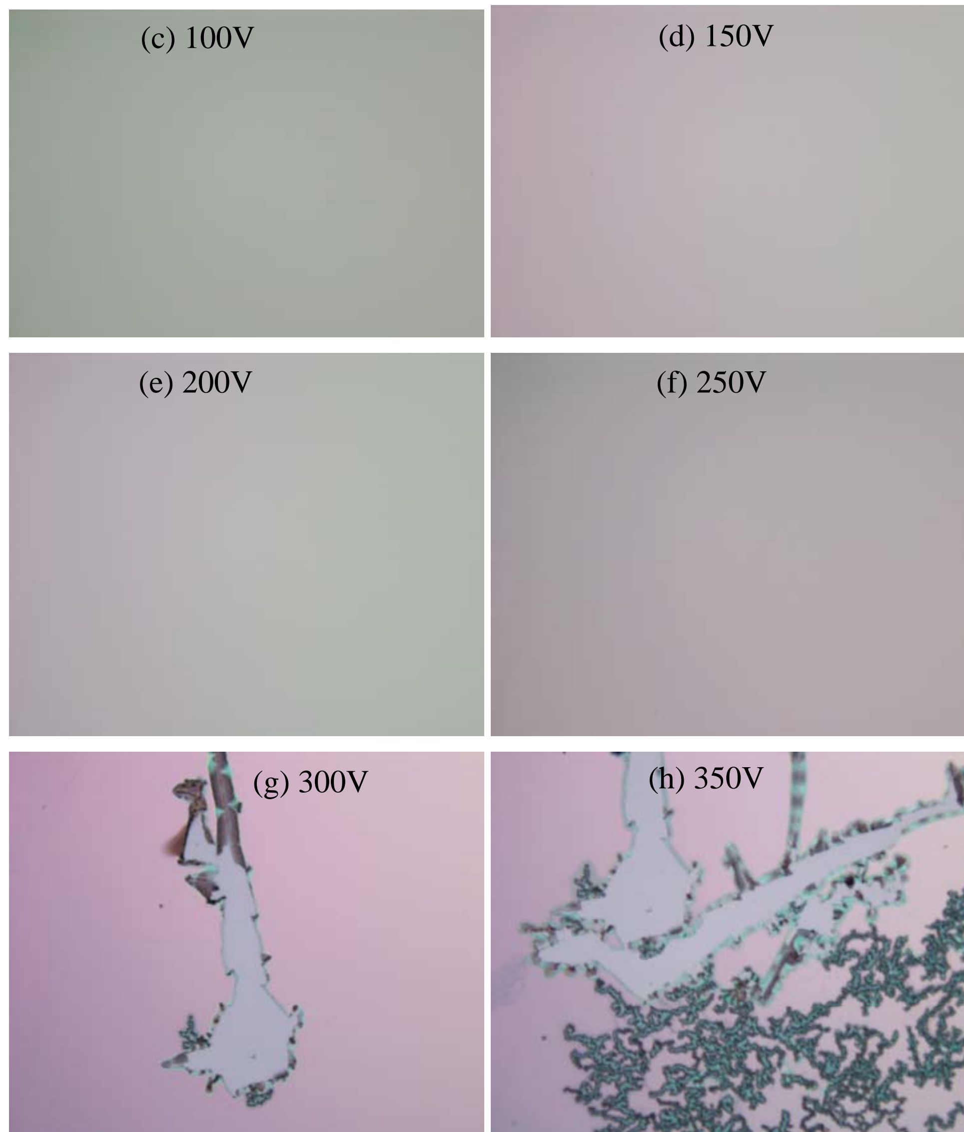

Figure 4. Optical images of capacitor after applied voltage from 0V to 350V.

Electrode Thickness

The effects of the electrode thickness on device performance and clearing are an important consideration. Comparisons of breakdown tests for capacitors with 100Å, 200Å and 300Å Al electrodes are shown in Figure 5. The clearing, discernable by the increased leakage current, originates at lower voltages for the thicker electrodes. The thicker electrodes also display higher leakage than the thinner the electrodes, indicative of more powerful clearing events. Figure 6 plots the capacitance vs. voltage for the same capacitors in Fig. 5. Due to the more energetic clearing, the 300Å electrode device begins loosing significant capacitance between 200V and 250V. The 200Å device first looses about 10% of the capacitance around 200V. This corresponds with the high energy clearing seen at around 180V, but the

capacitance remains stable after those events until above 250V. The 100Å capacitor maintains its value to above 300V. As with the 200Å capacitor, there is about 10% loss in capacitance due to isolated clearing around 280V prior to the primary clearing events. The difference in the initial capacitance of these devices is due to the shadow masking procedure during device processing. The higher deposition rate/longer deposition time for the thicker electrodes result in more spread beneath the edge of the mask and create a larger device area.

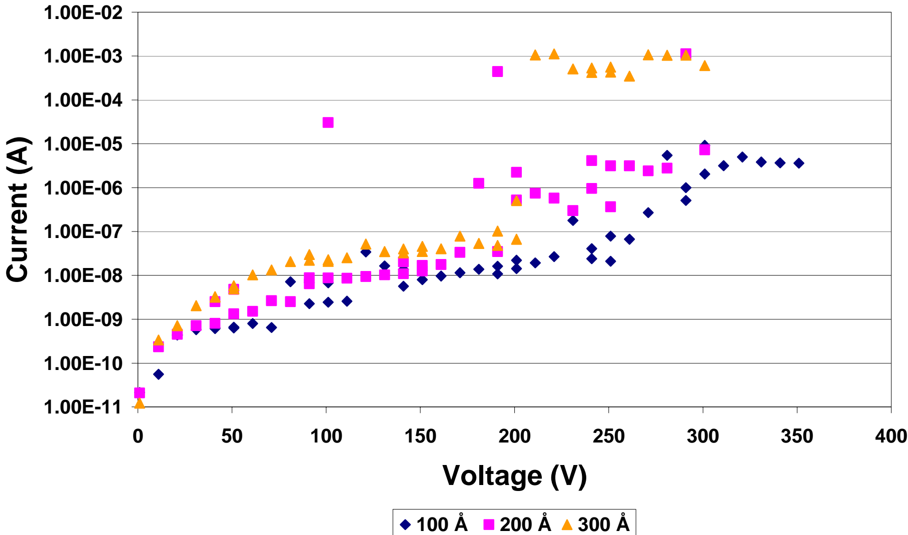

Figure 5. Effect of electrode thickness of capacitor leakage and clearing.

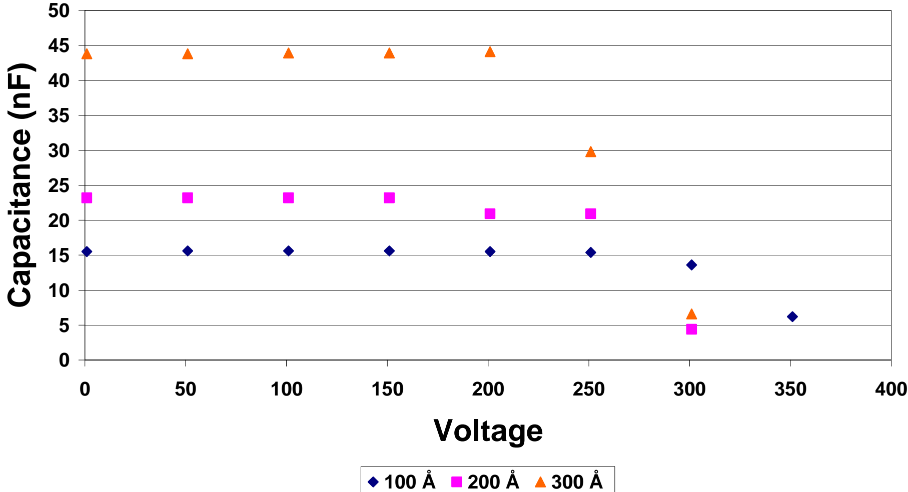

Figure 6. Capacitance vs. voltage for different electrode thicknesses.

Thermal Properties

The thermal response of the dielectric material is another important parameter for capacitor performance under extreme conditions. Figure 7 depicts the capacitance vs. frequency for a

wide temperature range under vacuum. The capacitance remains constant with frequency and is stable with increasing temperature to 300°C. As the temperature is increased above 300°C, the capacitance increases at low frequencies, while above 10 kHz no temperature effects are observed up to 400°C. The capacitance also remains stable under cryogenic conditions, with no variations observed down to -200°C. The differences in the capacitance between the elevated and cryogenic temperatures in Fig. 7 are due to differences in dielectric thickness between the samples measured. When capacitors are heated in ambient air, the capacitance at low frequency begins to increase around 200°C but still remains constant at high frequencies.

The dissipation factor is more temperature dependent than the capacitance. Under vacuum, significant increases in DF begin above 200°C while in air increases are observed around 150°C. No change in the dissipation factor is observed under cryogenic conditions. The difference between film performance in vacuum and in ambient air at elevated temperatures may be related to the atmospheric boundary layer present on the surface. Interactions with particulates in the atmospheric boundary layer over the top electrode may begin to alter the electric field as the temperature increases. The boundary layer is more pronounced in atmospheric air compared to vacuum environment and the temperatures effects are seen at lower temperatures. The temperature effects on both capacitance and dissipation factor are reversible. The original values are reacquired after returning the material back to room temperature and are stable after multiple temperature cycles. The high and low temperature values are also repeatably obtained on each temperature cycle. This indicates the observed capacitance and dissipation shifts are not caused by a chemical reaction, but by reversible interactions between the atmosphere and the surface.

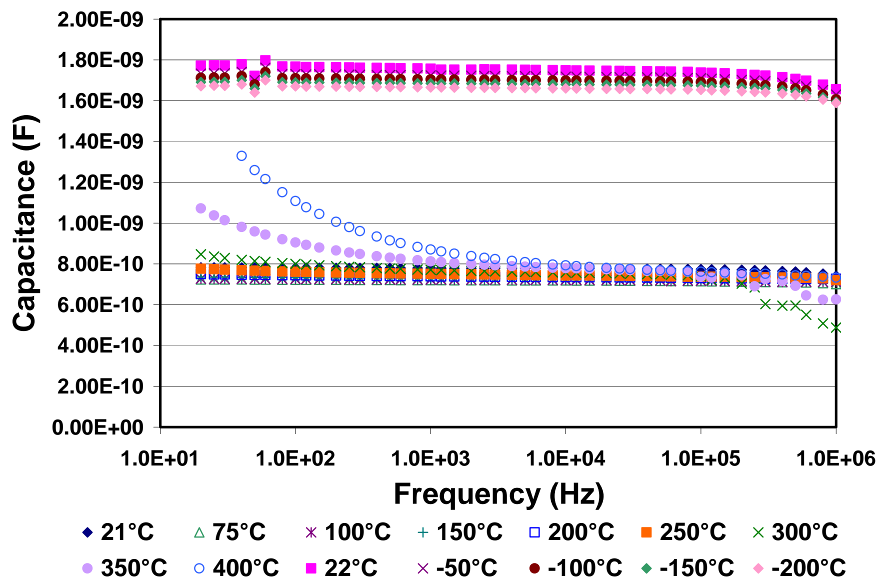

Figure 7. Effects of temperature on capacitance.

Conclusions

Aluminum oxynitride dielectrics for high energy density capacitors applications have been deposited using a pulsed DC magnetron sputtering technique. Multilayer capacitor structures

have been developed using in-situ deposition of alternating aluminum and aluminum oxynitride layers. Dielectric constants of ~9, with a dissipation factor less than 1% have been achieved. Thin aluminum electrodes have shown the ability to clear defects without significant loss of capacitance. Thinner electrodes maintain their capacitance to higher voltages and clear with less energy than thicker electrode devices. Clearing destroys the electrode connection at ~600 V/ m, but physical dielectric breakdown is not yet observed. The capacitance remains stable with temperature from -200°C to 400°C. The dissipation factor is more temperature sensitive and begins demonstrating temperature deviations above 200°C. The temperature effects are reversible and films regain their as-deposited properties when returned to room temperature.

References

[1] M. Rabuffi and G. Picci. “Status quo and future prospects for metallized polypropolene energy storage capacitors,” *IEEE Trans. Plasma Sci.*, **30**, 1939-1942 (2002).

[2] W.M. Yim, E.J. Stofko, P.J. Zanzucchi, J.I. Pankove, M. Ettenberg, and S.L. Gilbert. “Expitaxial grown AlN and its optical band gap,” *J. Appl. Phys.*, **44**, 292-296 (1973).

[3] R.D. Vispute, J. Narayan, and J.D. Budai. “High quality optoelectronic grade epitaxial AlN films on α-Al_2O_3, Si, and 6H-SiC by pulsed laser deposition.,” *Thin Solid Films*, **299**, 94-103 (1997).

[4] F. Martin, P. Muralt, M.-A. Dubois, and A. Pezous. "Thickness dependence of the properties of highly c-axis textured AlN thin films." *J. Vac. Sci. Technol. A,* **22**, 361-365 (2004).

[5] C.L Aardahl, J.W. Rogers Jr., H.K Yun, Y. Ono, D.J. Tweet, S.-T. Hsu. "Electrical properties of AlN thin films deposited at low temperature on Si(100)." *Thin Solid Films,* **146,** 174-180 (1999).

[6] K.K. Harris, B.P. Gila, J. Deroaches, K.N. Lee, J.D. MacKenzie, C.R. Abernathy, F. Ren, and S.J. Pearton. "Microstructure and thermal stability of aluminum nitride thin films deposited at low temperature on silicon." *J. Electrochem. Soc.,* **149**, G128-G130 (2002).

[7] V. Dimitrova, D. Manova, and E. Valcheva. "Optical and dielectric properties of dc magnetron sputtered AlN thin films correlated with deposition conditions." *Mater. Sci. Eng. B* **68**, 1-4 (1999).

[8] J. Schulte and G. Sobe. "Magnetron sputtering of aluminum using oxygen or nitrogen as reactive gas." *Thin Solid Films*, **324**, 19-24 (1998).

[9] J.-W Lee and S.C.N. Cheng. "Development of SiN_x and AlN_x passivation layers." *Thin Solid Films,* **358,** 215-222 (2000).

[10] K. Jagannadham, K. Sharma, Q. Wei, R. Kalyanraman, and J. Narayan. "Structural characteristics of AlN films deposited by pulsed laser deposition and reactive magnetron sputtering: A comparative study." *J. Vac. Sci. Technol. A* **16**, 2804-2815 (1998).

[11] T.T. Leung and C.W. Ong. “Nearly amorphous to epitxial growth of aluminum nitride films,” *Diamond Rel. Mater.* **13**, 1603-1608 (2004).

[12] J. Kolodzey, E.A. Chowdhury, T.N. Adam, G. Qui, I. Rau, J.O. Olowolafe, J.S. Suehle, and Y. Chen. “Electrical conduction and dielectric breakdown in aluminum oxide insulators on silicon,” *IEEE Trans. Electr. Dev.*, **47**, 121-128 (2000).

[13] K.R. Bray, R.L.C. Wu, S. Fries-Carr, and J. Weimer, “Aluminum oxynitride dielectrics for high power, wide temperature capacitor applications”, *CARTS USA 2006* , 161-170, (2006).

[14] K.R. Bray, R.L.C. Wu, S. Fries-Carr, and J. Weimer, “Aluminum nitride dielectrics for high energy density capacitors”, *Ceramic Transactions* 179, 45-55, (2006).

[15] L. Vu-Quoc, V. Srinivas, and Y. Zhai, “Finite element analysis of advanced multilayer capacitors,” *International Journal for Numerical Methods in Engineering*, **58**, 397 (2003).
[16] F. Engelmark, J. Westlinder, G.F. Iriarte,
I.V. Katardjiev, and J. Olsson. “Electrical characterization of AlN MIS and MIM structures,” *IEEE Trans. Electr. Dev.*, **50**, 1214-1219 (2003).

Acknowledgement

This research was conducted under K Systems Contract No. FA8650-04-C-2415 sponsored by OSD/AF for K Systems SBIR Phase II Program